Vol. 40 (2009) ACTA PHYSICA POLONICA B No 3

IN-BEAM GAMMA-RAY SPECTROSCOPY WITH RI BEAMS ON NEUTRON-RICH NUCLEI FAR FROM STABILITY*

M. Ishihara

RIKEN Nishina Research Center
Wako-shi, Saitama, 351-0001, Japan

(Received November 7, 2008)

Gamma-ray spectroscopy using intermediate-energy RI beams of projectile fragments has been useful for investigating low-lying states of extremely neutron rich nuclei far from the valley of stability. Coulomb excitation and proton inelastic scatterings are probing reactions most favorably employed, and problems of appearance/disappearance of magicity and emergence of new regions of deformation have been the central research objectives. In this paper, we first present a review on the novel features of the spectroscopic methods with RI beams, and then describe some of the highlights of such spectroscopic works recently performed at RIKEN.

PACS numbers: 21.10.–k, 21.10.Gv, 21.10.Re, 21.10.Tg

1. Introduction

In-beam gamma-ray spectroscopy was started in mid 60's when Morinaga and Gugelot observed E2 gamma-ray cascades along rotational bands in some of rare-earth deformed nuclei with (α,xn) reactions [1]. Since then the spectroscopy on rapidly rotating nuclei has been developed tremendously by exploiting the particular merit of heavy ion fusion reactions for efficiently populating high spin states. In recent years methods of in-beam gamma-ray spectroscopy have been extended to involve other types of reactions such as quasi-elastic [2] or deep inelastic scatterings [3] so that one can gain better access to uncultivated domains of nuclear chart. In particular in-beam gamma-ray spectroscopy incorporating RI beams was initiated at RIKEN in mid 90's [4] to open up a new paradigm of spectroscopy, which has greatly widened the research territory over a vast area far from the valley of stability.

* Presented at the Zakopane Conference on Nuclear Physics, September 1–7, 2008, Zakopane, Poland.

The methods of RI-beam gamma-ray spectroscopy are dictated by the characteristic properties of the secondary beams used. There are two types of RI beams; one being comprised of intermediate-energy projectile fragments (PF) and the other due to post accelerated ISOL beams. Our method employs PF RI beams, which are obtained at RIken Projectile-fragment Separator (RIPS) coupled to the $K = 540$ MeV ring cyclotron at RIKEN. By virtue of fairly intense RI beams from RIPS as well as novel techniques cultivated to facilitate efficient spectroscopy one can now apply the method over a broad region of unstable nuclei. In particular nuclei with large excess of neutrons may manifest intriguing features such as appearance/disappearance of magicity and/or emergence of new regions of deformation. The capability of the present method allows systematic studies on nuclear structure over long chains of isotopes, thereby clearly revealing those exotic features.

In Section 2 we review our methods of gamma-ray spectroscopy, which are so powerful as to facilitate the spectroscopy even for such rare isotopes as produced only at a rate of 1 pps or less. In Section 3 we discuss on some of recent results obtained with these methods, which cover the subjects such as (1) development of deformation towards $N = 40$ as indicated from the study of (p, p') on ^{60,62}Cr; (2) strongly suppressed B(E2) *vs.* fairly enhanced neutron collectivity of the 2^+ state in ^{16}C revealed by lifetime measurement and the study on (p, p'), indicating quenched E2 effective charges for neutron rich nuclei as well as growth of magicity at $Z = 6$; and (3) possible halo effects on a loosely bound deformed nucleus as manifested in the suppressed M1 strength and lowered excitation energy of the ^{17}C $1/2^+$ state.

2. Methods of gamma-ray spectroscopy with RI beams of projectile fragments

2.1. Unique features of the spectroscopic methods with PF RI beams

RI beams are secondary beams so that their intensities are often in the range of 10^0 to 10^5 particles per second (pps), which are far weaker than those of primary beams typically in the orders of 10^9 to 10^{12} pps. Accordingly any experimental methods with RI beams are demanded to incorporate novel means to enhance the experimental efficiency drastically.

In order to gain the efficiency our methods of gamma-ray spectroscopy are designed so as to fit to the characteristic features of the PF RI beams. Since the secondary beam particles are raw products from projectile fragmentation they carry almost the same intermediate energies as for the incident beams, and the associated beam emittance and energy resolution are considerably poor. One should also note the unique kinematical condition that the reactions with RI beams proceed in the inverse kinematics, *i.e.*, incident RI beam particles are those to be investigated while the target nuclei are those to probe the properties of the RI nuclei. Thus recoil nuclei of interest fly forward with fast velocities.

The properties of the PF RI beams are rather inferior. However they could be wisely employed as advantages or the aspects of demerits could be remedied by adequate counter means. Indeed their characteristic features are effectively employed to facilitate the gamma-ray spectroscopy as following: (1) Intermediate energies allow use of relatively thick targets and cause fairly strong Lorentz boost in the kinematics of outgoing particles. Both of these features serve to enhance the experimental efficiency greatly. (2) The poor energy resolution of RI beams hampers accurate determination of the excitation energies (E_x) by means of missing mass methods. However, incorporation of gamma-ray detection easily facilitates precise determination of E_x. (3) Demerits of the poor emittance can be remedied by tracking the trajectory of each particle, which is possible because of relatively weak beam intensities. (4) Recoil nuclei fly rapidly causing strong Doppler shifts, which can be well treated by using segmented gamma-ray detector array. (5) Inverse kinematics of reactions, where the target nuclei serve as probing particles, offer a special advantage that one can easily switch the types of reactions by simply changing the species of the target nuclei. This allows quick and easy accumulation of systematic data over different types of reactions. (6) It is appreciated to employ reactions with largest cross sections (σ) to compensate the demerit of weak beam intensity. The reactions which preferably occur at intermediate energies are mostly direct-type reactions while the fusion reaction no longer prevails. Among them we find the following two types of reactions to be very useful; one being the intermediate-energy Coulomb excitation (IE Coulex) [4] and the other the proton inelastic scatterings, (p, p') [5].

2.2. Spectroscopic methods with intermediate-energy Coulex and proton inelastic scatterings

Traditionally, one was recommended to work at incident energies well below the Coulomb barrier when one pursued sensible experiments with Coulex. This claim was asserted to maintain the condition that excitation due to electro-magnetic interaction should well overwhelm that due to nuclear interaction so that accurate strengths of electro-magnetic transitions can be extracted. In contrast, in the case of IE Coulex, one works with incident RI beams with intermediate energies which are far above the Coulomb barriers [4]. This departure, however, does not cause any deficiency as far as one employs target and projectile nuclei with sufficiently large atomic numbers (Z_{t} and Z_{p}). This is verified because of the strong dependence of Coulex cross section on $Z_{\rm t}$ and $Z_{\rm p}$ ($\sigma \propto Z_{\rm t}^2 Z_{\rm p}^2$) in contrast to the slow variation of the nuclear cross section. Note that the latter roughly goes like $(A_{\rm t}^{1/3} + A_{\rm p}^{1/3})$, where $A_{\rm t}$ and $A_{\rm p}$ respectively denote target and projectile mass numbers. Indeed, for the case of Pb target ($Z_{\rm t} = 82$) as often used practically, the Coulex cross section for an E2 transition well exceeds that due to nuclear interaction when $Z_{\rm p}$ is set to be larger than 10 or so. It is to be noted that use of Pb target serves not only to improve the Coulomb to nuclear ratio, but also to increase the magnitude of σ itself. For example, σ for the $0^+ \to 2^+$ Coulomb excitation in ^{32}Mg amounts to about 500 mb even at an intermediate energy of 50 MeV/u.

Another useful reaction for the spectroscopy is the proton inelastic scatterings, $(p,\, p')$ [5]. A unique advantage of this reaction arises from a trivial fact that one employs protons ($A_{\rm t} = 1$) for the target nuclei. The reaction rate is proportional to the number of atoms in the allowed thickness of target, which is in turn essentially proportional to $A_{\rm t}^{-1}$. Thus use of proton target tremendously enhances the reaction rate.

In Table I we compare the counting rates of γ-rays from the 2^+ state in ^{32}Mg between the two reactions employed, Coulex with a Pb target and the $(p,\, p')$ reaction. In these measurements the gamma rays are registered in coincidence with inelastically scattered ^{32}Mg particles off Pb nuclei or protons, which appear in a narrow cone of the forward angles. By detecting almost all of those particles rather easily the gamma-ray counting rates obtained essentially account for the angle-integrated total cross sections. Here the incident energies taken are about 50 MeV/u. The target thickness is a little thicker for Pb than for protons and σ is about 10 times larger for Coulex than $(p,\, p')$, while the same setup for γ-ray detection is used. Yet the net counting rate in $(p,\, p')$ much exceeds that for Coulex.

TABLE I

Counting rates for the $2^+ \to 0^+$ γ-rays in ^{32}Mg excited by Coulex and $(p,\, p')$, where the typical beam intensity of 0.8 kpps and γ-ray detection efficiency of 30% are assumed.

Reaction	σ [mb]	Target thickness [mg/cm^2]	$A_{\rm t}$	Counting rate [Hz]
Coulex	500	250	208	0.09
$(p,\, p')$	45	150	1	0.95

Most importantly, the rate amounts to about 0.1 Hz or 1.0 Hz, allowing about 10^4 or 10^5 events registered in a single day. Such a superb efficiency represents the power of the present method of RI beam gamma-ray spectroscopy.

2.3. Spectroscopy on shell evolution and development of deformation studied with intermediate energy Coulex and (p, p′)

Because of nature of the direct reactions both IE Coulex and $(p,\, p')$ reaction tend to result in only small amounts of energy and angular momentum transfers. Hence they are only efficient to populate low-lying states with low spins. Thus, for the cases of even–even nuclei, IE Coulex primarily populates the first 2^+ excited state (2^+_1), while $(p,\, p')$ populates the 2^+_1 state most favourably and the 4^+_1 state modestly. It is remarkable, however, that, in spite of the small number of states excited, the amount of spectroscopic information obtained is surprisingly rich. Indeed the study of Coulex could reveal not only E_x of the 2^+_1 state, but also the E2 transition strength between the ground 0^+ state and the 2^+_1 state, $B(\mathrm{E2}; 0^+\mathrm{g.s.} \to 2^+_1)$. Similarly the $(p,\, p')$ reaction may be used to determine the deformation length, δ, as well as the energy ratio, $R_{4/2} = E_x(4^+_1)/E_x(2^+_1)$.

Here one needs to pay small caution for the fact that the IE Coulex may loose its validity for accurate determination of $B(\mathrm{E2})$ when Z_{p} becomes very small ($Z_{\mathrm{p}} \lesssim 7$). An alternative means to determine $B(\mathrm{E2})$ for such light nuclei is to perform lifetime measurements. For this purpose we have recently developed a recoil shadow method (RSM) [6]. This method, which benefits from very high velocities ($v/c \sim 0.4$) of forward moving recoils, is useful to determine the mean lifetimes (τ) in the range of 10 ps to 1 ns. Thus it may be applied to some of M1 transitions as well as to a variety of E2 transitions.

The set of observables, $E_x(2^+_1)$, $E_x(4^+_1)$, $B(\mathrm{E2})$, and δ, as obtained from the Coulex and $(p,\, p')$ reactions provides substantial information on the degree of deformation (collectivity). Thus, by observing these quantities systematically, one can trace the features of growth/quenching of shell gaps (magicity) and manifestation of new region of deformation over a broad domain of unstable nuclei. Given the values of $B(\mathrm{E2})$ and δ, one can even determine the proton and neutron components of the E2 transition matrix separately [7], where the proton component $M_p(\mathrm{E2})$ is directly obtained from $B(\mathrm{E2})$ while the neutron component $M_n(\mathrm{E2})$ is given as a function of $B(\mathrm{E2})$ and δ. According to liquid model consideration, a relation of $M_n/M_p = N/Z$ is expected, while significant deviation may occur in extremely neutron-rich nuclei, representing heterogeneous nature of the nuclear system. Thus analysis based on $B(\mathrm{E2})$ and δ may be specially useful for nuclei far from stability.

3. Highlights of recent works of RI-beam γ-ray spectroscopy on neutron rich isotopes

3.1. Study of (p, p′) on ^{60,62}Cr and development of deformation towards $N = 40$

The neutron number of $N = 40$ is often considered to be a good magic number corresponding to the closure of p–f shells. One of the intriguing possibilities unique to neutron-rich nuclei is occurrence of dramatic changes of shell structure, which may be caused by different reasons such as due to tensor interaction [8] or weakened ls interaction [9]. Such a change of shell structure may result in disappearance of traditional magic numbers, hence promoting quenching of shell closure eventually to induce new deformed region around the old magic number. A notable example of such an anomaly is found in the region around ^{32}Mg with $N = 20$ (Island of Inversion), where large deformation is well manifested as revealed by the first experiment by means of IE Coulex [4]. Such studies on disappearance of magicity have now been extended towards heavier regions. Our recent work [10] aimed to examine the shell quenching around $N = 40$ by investigating signatures of deformation in the neighboring chromium (Cr) isotopes.

Cr isotopes have two advantages to study the features of shell evolution/emergence of new deformed regions: Firstly their atomic number $Z = 24$ corresponds to half occupancy of the $f_{7/2}$ proton shell so that relatively strong tendency towards deformation is expected. This feature may serve to enhance the development of deformation in a new region if any. Secondary the Cr isotopes are experimentally accessible over a wide range of neutron number starting from the vicinity of $N = 20$ to that of $N = 40$. Systematic studies over such a long chain of isotopes should be effective to reveal varying natures of nuclear structure.

So far experimental data of $E_x(2_1^+)$, $E_x(4_1^+)$ and δ are available for the whole Cr isotopes between $N = 22$ to $N = 34$, while δ is not known for ^{60}Cr ($N = 36$) and only $E_x(2_1^+)$ is known for ^{62}Cr ($N = 38$). The energy ratio of $R_{4/2} = E_x(4_1^+)/E_x(2_1^+)$ provides a good measure of deformation since the ratio tends to increase with growing deformation from the vibration limit of 2.0 towards 10/3 for a solid rotor. The data of δ also provides a good measure of deformability since it represents the magnitude of E2 collectivity. As described in Sect. 2.3 the $(p,\, p')$ reaction is powerful to determine both $R_{4/2}$ and δ. We therefore observed the $(p,\, p')$ reactions on ^{60}Cr and ^{62}Cr at the incident energy of about 40 MeV/u so that trends of deformation can be traced up to the heavier isotopes closer to $N = 40$. The efficiency and S/N ratio of the measurements were much improved by using a target of liquid hydrogen with thickness of 72 mg/cm^2. Indeed both the $4_1^+ \to 2_1^+$ and $2_1^+ \to 0^+$ g.s. transitions were clearly observed in both of the reactions, and the $E_x(4_1^+)$ value of 1180(11) keV was newly found for ^{62}Cr. The angle-integrated cross section for exciting the 2_1^+ state was also obtained for both of the isotopes, yielding deformation lengths of 1.12(16) fm and 1.36(14) fm, respectively, for ^{60}Cr and ^{62}Cr.

The results of δ, E_x and $R_{4/2}$ for ^{60}Cr and ^{62}Cr are shown in Fig. 1 together with the data for the other Cr isotopes. The deformation length δ gradually increases as the isotope moves from $N = 32$ to 38, indicating growing collectivity towards $N = 40$. The behavior of $R_{4/2}$ is in harmony with that of δ, exhibiting a gradual increase towards $N = 40$. The $R_{4/2}$ value of 2.7 at ^{62}Cr is fairly close to 10/3, indicating that this isotope bears significant deformation.

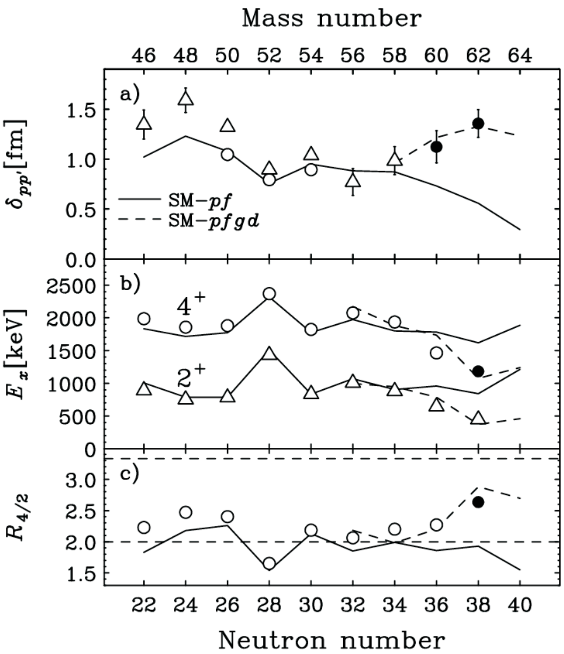

Fig. 1. Comparison of deformation length ($\delta_{pp'}$), excitation energies ($E_x(2_1^+)$ and $E_x(4_1^+)$), and energy ratio ($R_{4/2} = E_x(4_1^+)/E_x(2_1^+)$) over a long chain of Cr isotopes ranging to ^{62}Cr.

The experimental results are compared with two shell model calculations [11], one with its model space truncated to pf shells (SM-pf) and the other with its model space expanded to pf and gd shells (SM-$pfgd$). The experimental results are well reproduced with SM-pf for the region from $N = 28$ to 34. On the other hand deviation becomes evident at $N = 36$ and more significant at $N = 38$ while they are better reproduced with SM-$pfgd$. The theory of SM-$pfgd$ accommodates some features of shell gap quenching between the pf and gd shells. Thus the good agreement with the latter theory supports the hypothesis that the deformation is promoted in the Cr isotopes near $N = 40$ due to shell quenching for neutron-rich nuclei.

3.2. Hindered proton- vs. ordinal neutron- E2 transition strengths for the $2_1^+ \to 0^+$ g.s. in ^{16}C

In an earlier paper [6] we reported the result of lifetime measurement on the $2_1^+ \to 0^+$ g.s. transition in ^{16}C, which indicated an extremely suppressed B(E2) value invoking a variety of theoretical conjectures to account for the anomaly. In order to examine this phenomenon more closely we have newly performed two sets of measurements: (1) a renewed set of lifetime measurements on the 2_1^+ state of ^{16}C [12], and (2) observation of the (p, p') reaction on ^{16}C to determine δ for the 0^+g.s. $\to 2_1^+$ excitation [13]. Below I summarize the results from these studies, and discuss their implications on the intriguing $2_1^+ \to 0^+$ g.s. transition in ^{16}C.

In the renewed lifetime measurements with RSM, an upgraded setup with increased number of detector layers was employed to gain the accuracy and efficiency considerably. Moreover the lifetime was measured in three different reactions to confirm consistency. The mean lifetime (τ) thus determined was 18.3(14) ps, which is about 4 times shorter than the earlier result [6]. Using the revised value one obtains $B(\mathrm{E2}; 0^+\mathrm{g.s.} \to 2_1^+) = 13.0(10)$ e^2 fm^4.

In order to find significance of the new result we compare it with B(E2) values of other even–even nuclei up to $A = 55$ in Fig. 2, where B(E2) values are shown either in Weisskopf unit (upper panel) or as the ratio to the systematic value B_{sys} (lower panel) [14]. Here B_{sys} is given as $B_{\mathrm{sys}}(\mathrm{E2}; 0^+\mathrm{g.s.} \to 2_1^+) = 3.26(E_x[\mathrm{keV}])^{-1}Z^2A^{-0.69}$ [e^{2}b^2], well reproducing global trends of B(E2) with respect to E_x, A and Z. We notice from these panels that there are at least two categories of nuclei whose B(E2)'s are strongly hindered; (a) double-magic nuclei such as ^{16}O, ^{40}Ca, ^{48}Ca, and (b) extremely neutron-rich single-magic nuclei such as ^{20}O and ^{22}O. We find that the B(E2) value of ^{16}C is even smaller than any of those hindered transitions as evident in the lower panel of Fig. 2. Thus even after the revision of the data the case of ^{16}C represents an abnormally hindered E2 transition.

In turn, the (p, p') reaction on ^{16}C at 33 MeV/u revealed $\delta = 1.44 \pm 0.17$ fm. By combining with B(E2) and applying the recipe mentioned in Sect. 2.3 one can determine the proton and neutron E2 transition matrices separately as $M_p = 3.6 \pm 0.5$ fm^2 and $M_n = 11 \pm 2$ fm^2. One then obtains $M_n/M_p = 3.1 \pm 0.7$, which is much larger than $N/Z = 10/6$ as expected from the liquid drop argument. It is interesting to note that the neutron matrix is fairly large to be almost compatible with the expectation value from the systematics [14]. Thus suppression of E2 transition matrix in ^{16}C occurs strongly for protons but not at all for neutrons.

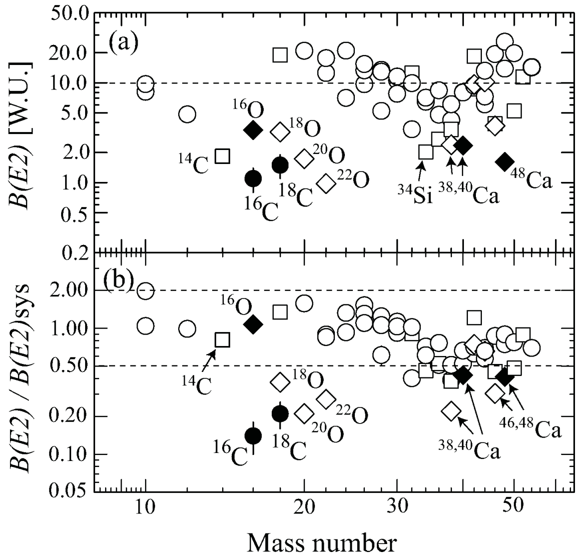

Fig. 2. Comparison of $B(\mathrm{E2}; 0^{+}\mathrm{g.s.} \rightarrow 2_1^+)$ for even–even nuclei over a region ranging to $A = 55$ in terms of the value in Weisskopf unit (upper panel) and the ratio to B_{sys} [14] (lower panel).

There are several attempts to explain the suppressed $B(\mathrm{E2})$ of $^{16}\mathrm{C}$ in terms of shell model [15]. In such analysis E2 matrix elements (A_n, A_p) are calculated in a truncated shell space so that they can be related to the true matrices (M_n, M_p) only by introducing effective charges: $eM_p = (e_p^{\mathrm{eff}} A_p + e_n^{\mathrm{eff}} A_n)$ and $eM_n = (e_p^{\mathrm{eff}} A_n + e_n^{\mathrm{eff}} A_p)$. By using the values of $A_p = 1.05$ fm^2 and $A_n = 7.58$ fm^2 as calculated with SFO interaction [16] one can figure out the proper magnitudes of the effective charges. Here the extremely small value of A_p as compared to A_n partly represents the effect of enhanced shell gap (growth of magicity) at $N = 6$ for this neutron-rich isotope of $^{16}\mathrm{C}$. By using the standard set of $e_p^{\mathrm{eff}} = 1.3e$ and $e_n^{\mathrm{eff}} = 0.5e$ one obtains $B(\mathrm{E2}) = 26.6$ e^{2}fm^4, which is about 2 times larger than the experimental value. On the other hand significant quenching of effective charges is expected for nuclei with large excess of neutrons [17, 18]. By using reduced values of $e_p^{\mathrm{eff}} = 1.16e$ and $e_n^{\mathrm{eff}} = 0.33e$ as expected from such arguments one obtains $B(\mathrm{E2}) = 13.8$ e^{2}fm^4, which is very close to the observed value. Thus the effect of quenched effective charges is crucial for this neutron rich isotope of $^{16}\mathrm{C}$. It is conceivable that the extremely reduced E2 strengths as found in several neutron-rich single-magic nuclei (see Fig. 2) may be as well attributed to such effects of the e^{eff} quenching.

In contrast, a recent paper argues that the result of ^{16}C may be well explained with an ordinary value of e^{eff} [19]. However that argument simply assumes vanishing value of A_p, which may easily alter the calculated B(E2) result by factor of 2 or so.

3.3. Possible halo effects on loosely bound deformed nuclei as manifested in the $1/2^+$ state in ^{17}C

The ^{17}C isotope is unique in that the spin-parity of the ground state is $3/2^+$ while spherical nuclei with $N = 11$ usually exhibit $5/2^+$, corresponding to the occupancy of $1d_{5/2}$ orbital with their valence neutrons. This anomalous spin-parity is common to another $N = 11$ isotone ^{21}Ne, which is known to be a deformed nucleus. Furthermore these two nuclei share another feature that two of the lowest lying excited levels are $5/2^+$ and $1/2^+$ states. Thus it is probable that the ^{17}C isotope is a deformed nucleus as well.

In our recent work [20], we performed lifetime measurements for these low-lying states of ^{17}C using the upgraded RSM [12], and obtained $\tau = 583 \pm 21$(sta)± 35(syst) ps and $\tau = 18.9 \pm 0.6$(sta)± 4.7(syst) ps, respectively, for the first excited state of $1/2^+$ at 212 keV and the second excited state of $5/2^+$ at 333 keV. The relevant γ transitions de-exciting to the ground states are considered to be M1 transitions, and the B(M1) values in unit of $10^{-2}\mu_N^2$ are deduced to be 1.0 ± 0.1 and $8.2^{+3.2}_{-1.8}$, respectively.

In Fig. 3 we compare level schemes of ^{17}C and ^{21}Ne, where E_x and B(M1) are shown together. It is remarkable that both the values of E_x and B(M1) are quite similar between the two nuclei as far as the $5/2^+$ state is concerned. In contrast the behavior of the $1/2^+$ state is considerably different between the two nuclei, exhibiting values of E_x and B(M1) extremely reduced for ^{17}C as compared to those for ^{21}Ne: The E_x is lowered by more than 2.5 MeV, and the B(M1) is suppressed by more than 30 times.

A possible origin of this anomaly may be attributed to halo effects on a loosely bound deformed nucleus. As a matter of fact ^{17}C is a very loosely bound nucleus with neutron separation energy S_n as small as 729 keV while ^{21}Ne is well bound nucleus with $S_n = 6761$ keV. According to Hamamoto, a Nilsson orbital of $\Omega = 1/2^+$ tends to become dominated by the s-component in the spherical bases while losing amplitudes for the d-components as its binding energy becomes smaller towards the threshold for separation [21]. Accordingly a loosely bound $\Omega = 1/2^+$ orbital would somewhat regain its binding energy because of the promoted radial extension, and would give rise to a considerable loss in the M1 strength of the transition leading to the d-dominant $3/2^+$ ground state. These halo effects are exclusively expected for a loosely bound $\Omega = 1/2^+$ orbital, while they indeed account for the observed anomalies for the $1/2^+$ state qualitatively.

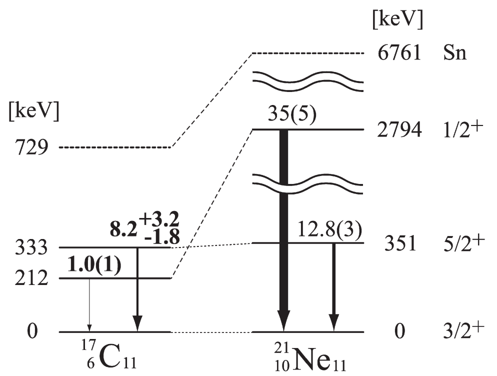

Fig. 3. Comparison of level schemes between two $N = 11$ isotones of ^{17}C and ^{21}Ne. The values of E_x and B(M1) are shown together.

In a recent paper [22], a different possibility is argued that the $1/2^+$ state in ^{17}C is due to a $K = 1/2^+$ orbital with oblate shape. In that scenario, the suppressed B(M1) is attributed to shape difference between the initial $1/2^+$ and final $3/2^+$ states.

The author is grateful to Dr. D. Suzuki for his cooperation in completing the paper. He is also grateful to Drs. N. Aoi. H.J. Ong and T. Motobayashi for their useful scientific inputs.

REFERENCES

[1] H. Morinaga, P.C. Gugelot, *Nucl. Phys.* **46**, 21 (1963).
[2] T. Inamura, M. Ishihara *et al.*, *Phys. Lett.* **B68**, 51 (1977).
[3] R. Broda *et al.*, *Phys. Rev. Lett.* **68**, 1671 (1992).
[4] T. Motobayashi, M. Ishihara *et al.*, *Phys. Lett.* **B346**, 9 (1995).
[5] H. Iwasaki, M. Ishihara *et al.*, *Phys. Lett.* **B481**, 7 (2000).
[6] N. Imai *et al.*, *Phys. Rev. Lett.* **92**, 062501 (2004).
[7] A. Bernstein *et al.*, *Phys. Rev. Lett.* **42**, 425 (1979).
[8] T. Otsuka *et al.*, *Phys. Rev. Lett.* **95**, 232502 (2005).
[9] J. Dobaczewski *et al.*, *Phys. Rev. Lett.* **72**, 981 (1994).
[10] N. Aoi *et al.*, *Phys. Rev. Lett.* **102**, 012502 (2009).
[11] M. Honma *et al.*, *Phys. Rev.* **C69**, 034335 (2004) and private communication.
[12] H.J. Ong *et al.*, *Phys. Rev.* **C78**, 014308 (2008).
[13] H.J. Ong *et al.*, *Phys. Rev.* **C73**, 024610 (2006).

[14] S. Raman *et al.*, *Phys. Rev.* **C37**, 805 (1997).
[15] *E.g.*, A. Umeya *et al.*, *Phys. Rev.* **C77**, 044301 (2008).
[16] T. Otsuka *et al.*, *Phys. Rev. Lett.* **87**, 082502 (2001).
[17] H. Ogawa *et al.*, *Phys. Rev.* **C67**, 064308 (2003).
[18] H. Sagawa, K. Asahi, *Rhys. Rev.* **C63**, 064310 (2001).
[19] M. Wiedeking *et al.*, *Phys. Rev. Lett.* **100**, 152501 (2008).
[20] D. Suzuki *et al.*, *Phys. Lett.* **B666**, 222 (2008).
[21] I. Hamamoto, *Phys. Rev.* **C69**, 041306(R) (2004).
[22] H. Sagawa *et al.*, *Phys. Rev.* **C78**, 041304(R) (2008).